The Build-Up of Droplet/Aerosols Carrying the SARS-CoV-2 Coronavirus, in Confined Spaces

Björn Birnir*
Center for Complex and Nonlinear Science
Department of Mathematics
University of California, Santa Barbara
Santa Barbara, CA 93106
and
Luiza Angheluta
The Njord Centre, Department of Physics
University of Oslo, P. O. Box 1048, 0316 Oslo, Norway

July 2020

Abstract

A model of the distribution of respiratory droplets and aerosols by Lagrangian turbulent air-flow is developed and used to show how the SARS-CoV-2 Coronavirus can be dispersed by the breathing of an infected person. It is shown that the concentration of viruses in the exhaled cloud can increase to infectious levels with time, in a confined space where the air recirculates. The model is used to analyze the air-flow and SARS-CoV-2 Coronavirus build-up in a restaurant in Guangzhou, China [17, 16]. It is concluded that the outbreak of Covid-19 in the restaurant in January 2020, is due to the build-up of the airborne droplets and aerosols carrying the SARS-CoV-2 Coronavirus and could not have been prevented by standard air-conditioning.

1 Introduction

The understanding of the mechanism of infection by the Covid-19 coronavirus has evolved considerably since the beginning of the pandemic. It is believed that the most common form of transmission is by respiratory droplets containing the coronavirus. These droplets were classically divided into heavier droplets that settle at a limited distance around the infected individual and aerosols (or droplet nuclei) that can remain airborn for an extended period and are convected by air inside confined spaces. The more recent scientific understanding is more nuanced. The pathogen-containing droplet can be carried by a turbulent cloud, emitted when the infected person coughs or sneezes.

*and the University of Iceland, School of Natural Sciences, 107 Reykjavík, Iceland

The droplets are active particles in this turbulent cloud and interact with the turbulent air and with each other. Experiments show that the cloud can rapidly spread up to a distance of 7-8 meters [11, 22, 12] (up to 25 feet). The droplet cloud, that is carried by air and can be airborne for hours, overlaps the artificial boundary of droplets and aerosols. We will adopt the terminology *droplet/aerosols*, in this paper, for droplets and aerosols around $5-10$ micrometers in diameter. This term will apply to all droplets and aerosols that are airborne for times greater than $1-10$ minutes, that carry the coronavirus and are a source of contagion.

There is mounting evidence that droplet/aerosols are an important source of contagion, in confined spaces. This makes it important to establish models that allow a computation of the concentration of the droplet/aerosols and how that concentration evolves over time. Such models would allow a computation of the risk of contagion and develop methods for its mitigation. In this paper we develop such a model based on Lagrangian fluid dynamics of turbulent air-flow. Then we use it to analyze an outbreak of infection [17] in a restaurant in Guangzhou, China, and compare with a numerical and experimental study [16] of the same outbreak.

Our study shows that the concentration of the droplet/aerosols may increase significantly in a confined space in the span of one hour. This increase in concentration is the likely cause of the outbreak in the restaurant in Guangzhou, China, see [17] and [16]. As discussed in [20] this increased concentration may spread by air-conditioning ducts from one confined space to another. The remedy is to greatly increase the effectiveness of the air-conditioning, see [20], or create a through flow through the confined space that washes the droplet/aerosols away. Applying such methods in confined spaces such as restaurants, offices, buses and classrooms, may dramatically decrease the contagion rates.

2 Lagrangian Turbulence and Structure Functions

The difference between the Eulerian and the Lagrangian description of fluid flow is the frame of reference of the observer (measurements) of the flow. In the Eulerian description the observer is stationary and the fluid flows by him or her. In the Lagrangian frame of reference the observer travels with the flow and make his measurements in this traveling frame of reference. The mathematical description in the Eulerian frame is the conventional Navier-Stokes equation, but in the Lagrangian frame it is the Navier-Stokes equation with the material derivative $\frac{Du}{DT} = \frac{\partial u}{\partial t} + u \cdot \nabla u$ where the time variable T is the Lagrangian time, u is the fluid velocity and t the Eulerian time. The Lagrangian description is natural for the droplet/aerosols transmission, since the natural frame of reference is the one traveling with the droplet/aerosol, to see where it originates and where it ends up.

The Eulerian description is the traditional description of homogeneous turbulence, see [5, 14], and boundary turbulence, see [24, 9]. When particles or fluid droplets, such as the droplet/aerosols carrying the coronavirus, are entrained in the (air) flow, the Lagrangian description is more appropriate. We want to travel with (in the frame of reference of) the turbulent cloud and see how the droplet/aerosols interact with the cloud and each other. We want to determine if and where the droplet/aerosols settle on the ground or on surfaces, or if they remain airborn. In the latter case, we want to determine to what destinations they are carried by the turbulent flow of air. The strength of the turbulence in the flow is given by the dimensionless Reynolds number $Re = \frac{uL}{\nu}$, where L is a typical spacial dimension of the flow and ν is the kinematic viscosity. In practice, one uses the

Taylor-Reynolds number $Re_\lambda = \frac{u\lambda}{\nu}$, where λ is the correlation length in the flow. We will use the approximation $Re_\lambda \approx \sqrt{10Re}$.

To compute the Richardson probability density function (PDF), see Appendix A, for the droplet/aerosols that are passive scalars we must construct the Lagrangian velocity structure functions (LVSF) [23, 2],

$$S_p(\tau) = \langle |u(T+\tau) - u(T)|^p \rangle = \langle |\delta u|^p \rangle,$$

for $p = 2$, where τ is a temporal lag-variable measuring the time passed between two observations of the flow, and $\langle \cdot \rangle$ is an ensamble average over many measurements.

The Kolmogorov-Obukhov theory determines the scaling laws in Lagrangian turbulence, for small τ,

$$S_p \sim \tilde{C}_p (\varepsilon\tau)^{p/2},$$

see [19, 18], where ε is the dissipation rate in the flow, and $\tilde{C}_p$ are constants, that are not universal, but depend on the configuration of the flow. In particular, for $p = 2$, we get $S_2 \sim \tilde{C}_2 \varepsilon\tau$, see [23]. Although the Lagrangian turbulent flow follows these scaling laws for τ sufficiently small, it quickly deviates from the predicted scaling exponents and approaches values of the scaling exponents that are more similar to their values in Eulerian turbulence [23]. In between, there is a "passover" interval where the values of the exponents dip significantly below either their initial or eventual values, see [23].

From a physical standpoint it is reasonably well understood what is going on. Initially, the mixing processes in Lagrangian turbulence cause the droplets to separate in a "super-diffusion" much faster than usual diffusion and obeying the Richardsson 4/3 law [21]. It says that the diffusivity is proportional to $\varepsilon r^{4/3} = \varepsilon\tau^2$, where r is the distance between the droplets. But later the turbulent eddies in the Richardson cascade have developed, as they they do in Eulerian turbulence, see [5], the droplets are entrained by these eddies and this leads to a slower diffusivity. However, the diffusivity is still much larger than in ordinary diffusion. The problem is that how you pass from one region, measured by r, "the Lagrangian" to the other "the Eulerian" is still not very well understood. This has blocked theoretical progress in Lagrangian turbulence. In other words, when describing droplet distribution, you cannot stay with the pure Lagrangian description, even at moderate separations r between droplets, you have to mix the Lagrangian with the Eulerian description.

In [9] the authors encountered a similar "passover region". This was the buffer region separating the viscous from the inertial layer in pipe and boundary turbulence. In the buffer region the variation (fluctuation squared) behaved very differently than in either the viscous or the inertial layer. They were able to overcome this obstacle by adapting a "spectral function" introduced in [13] to compute the mean velocity in boundary and pipe flow, and generalize it to also model the buffer layer. In [2], they adapt these methods to compute the Lagrangian velocity structure functions. We use the results for $S_2 = \langle |\delta u|^2 \rangle$, below.

3 Application to Covid-19

In a recent paper [17] the infection of 3 families by one infected person in an air-conditioned restaurant in Guangzhou, China, is described, see Figure 1. One of the families had travelled from Wuhan and ate lunch in the restaurant where the other two families were present. The first family

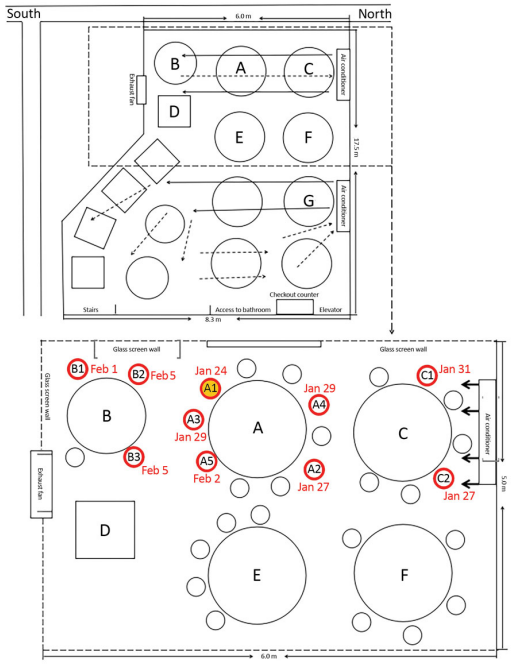

Figure 1: A sketch showing the arrangement of restaurant tables and air conditioning airflow at the site of an outbreak of 2019 coronavirus, in Guangzhou, China, 2020. Red circles indicate where patients that developed the disease were located; yellow-filled red circle (A1) indicates the location of the infected patient. The figure is taken from [17].

contained one person (A1) who fell ill later the same day and went to the hospital. 12 days later 9 other members of the three families had fallen ill with Covid-19. The infection is consistent with droplet transmission because no one else at the restaurant nor the servants fell ill. Only the persons in the direct airstream of the air-conditioner fell ill.

In the following we will use the above theory to simulate the dispersion of the droplet/aerosols in the restaurant. The part of the restaurant where the contagion took place is of dimensions 6 meters length and 3 meters width, see Figure 1. Air-conditioners are set so that the restaurant guest experience wind air blowing at the velocity of 0.25 meters per second, see [1]. The corresponding Taylor-Reynolds number is $Re_\lambda = 705$, since the air is flowing along a 3 meter distance from Table A to the wall where the air-conditioner is located. The three meter distance, perpendicular to the air-flow, is taken to be the distance across the largest table, where the infected person was sitting, and including one half-meter for each person sitting on opposite sites. Using the energy dissipation $\varepsilon = 1.2$, taken from the experimental and simulation data in [6], we get the Kolmogorov time scale $\tau_\eta = 3.55$ ms (milliseconds). We employ the theoretical structure function S_2 from [2] and use the stochastic closure theory (SCT), see [7, 8, 10], to compute the coefficient C_2 in the exponential of the formula for the Richardson distribution (A.1). This computation, that interpolates the coefficients computed in [14] for the Reynolds number $Re_\lambda = 705$, is explained in Appendix B.

The results of the simulations for the restaurant in Guangzhou are shown in Figures 2-6. In Figure 2 we show the Richardson distribution as a function of time and space. We assume that the infected person exhales 5 times a minute and each exhale event last 1.2 seconds, or 1/10 of the breathing period that is 12 seconds. Each time unit is $\tau_\eta = 3.55$ ms, and we are computing 2000

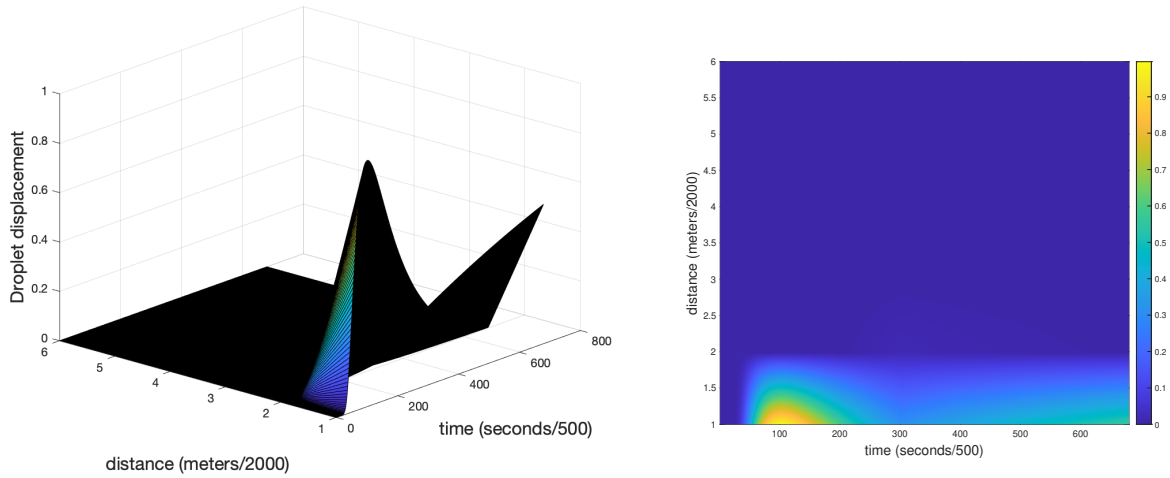

Figure 2: The Richardson distribution for the particle separation.

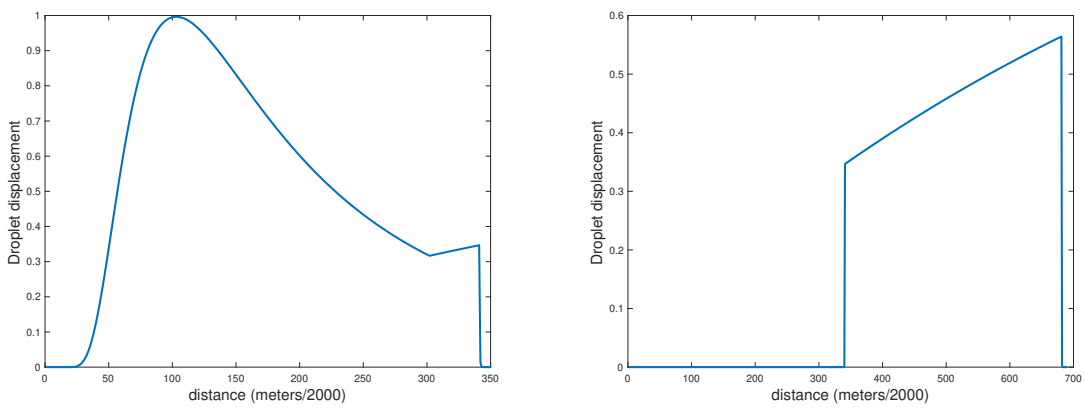

Figure 3: The initially exhaled (left) and subsequently propagated (right) spatial distributions of droplet displacement.

units for a total of 7.1 seconds. In the left figure in Figure 3, we show the complete distribution for one exhaling event, roughly 340 points $\approx$ 1.2 second. Observe that the distance between the points is greater in the beginning (Richardson dispersion) but becomes smaller after the exhale event (Eulerian diffusion). We make this clearer in Figure 3, where on the left we plot the distribution of the cloud for first 340 points or 1.2 seconds and on the right for the subsequent 340 point or the subsequent 1.2 seconds, to see what happens to the cloud immediately afterwards. We call the left the Lagrangian part and the right the Eulerian part of the exhale and propagation events. The cloud is clearly more diffuse during the Lagrangian part (Richardson dispersion) and more concentrated during the Eulerian part. The concentration of the droplet/aerosols is slightly (1.15 times) greater during the Eulerian phase. The cloud is traveling with the airflow, at 0.25 m/s, so the total length of the cloud is 0.3 meters, the Lagrangian part extends to 0.3 meters and the Eulerian part covers the subsequent 0.3 meters. Somewhat surprisingly the droplet/aerosol concentration within the first 0.3 meters is slightly less (0.87 times) than that at the 0.3 to 0.6 meters distance.

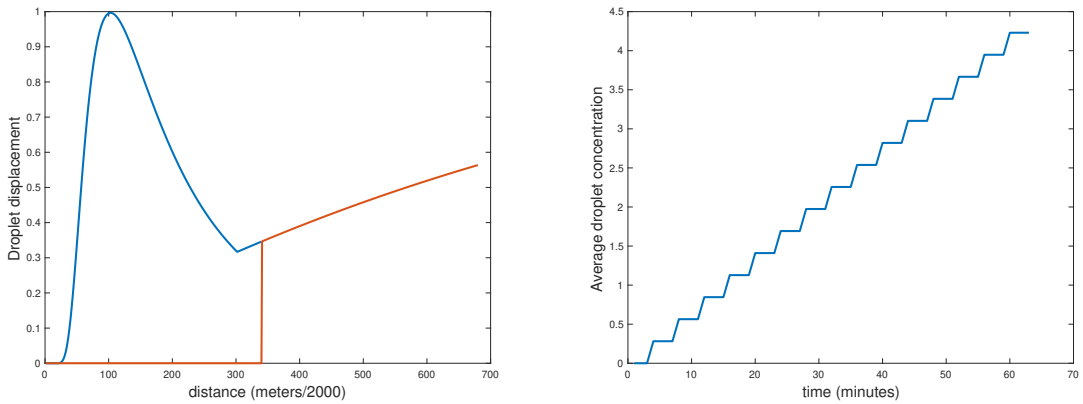

Figure 4: (Left) The total distribution of droplet displacement after 1.2 second of exhaling. This is the shape of the exhaled cloud and its subsequent propagation, up to 2.4 second. (Right) The average, in space (inside the pyramid), droplet concentration as a function of time, in minutes, normalized by the concentration at the infected person.

One can make a rough estimate of how the concentration of the droplet/aerosols builds up in time using the above theory and the CFD simulations shown in Figure 5. The volume of the whole space containing the contamination is 3 by 6 by 3.14 meters $=$ 56.52 m^3, see [16]. A pyramid with base on the wall opposite the air-conditioner mostly contains the blue contamination cloud, see Figure 5. Thus the cloud has roughly the volume $56.52/3 = 18.84\, m^3$. The radius of a cylinder containing the exhaled cloud, is the height of the cloud, and reaches its maximum at 100 units on the left figure in Figure 3. This corresponds to 0.35 seconds and the velocity determining the spread is probably not the velocity at which the cloud is drifting but the velocity with the droplets-aerosols are being ejected. This is taken to be 1.5 m/s in [16] and we will use the same value here. This give the radius 1.5 times 0.35 = 0.53 meters. If we let the exhaled clouds be contained in a cylinder with this radius extending the length of the contamination area we get the volume 5.33 m^3 for this cylinder. The droplet/aerosols in the cylinder now get spread to the pyramid, by the air-conditioning and heat conduction, see Figure 6. This decreases their concentration by a factor of $14.13/5.33 = 3.54$. However, the infected person keeps exhaling a new droplet/aerosol cloud every 12 seconds and since the extent of these clouds is 0.3 meters he needs to exhale 20 clouds to fill the 6 meter long cylinder. This takes 240 seconds or 4 minutes. In one hour he has filled the cylinder 15 = 60/4 times. Thus with no droplet/aerosols lost, the exhaust fan was closed see [16], the resulting concentration in the pyramid is $15 \times 1/3.54 = 4.23$ times what it was in the cylinder, the first time it was full. In other words, the concentration for everyone sitting at the three tables A, B and C, in Figure 1, in less than 15 minutes, is what it would be if they were sitting next to the infected person. In one hour, the concentration is more than four times what it was initially, if every person on the three table was sitting next to the infected person. This build-up of the concentration of the droplet/aerosols containing the SARS-CoV-2 virus is the likely reason for the outbreak in the restaurant in Guangzhou.

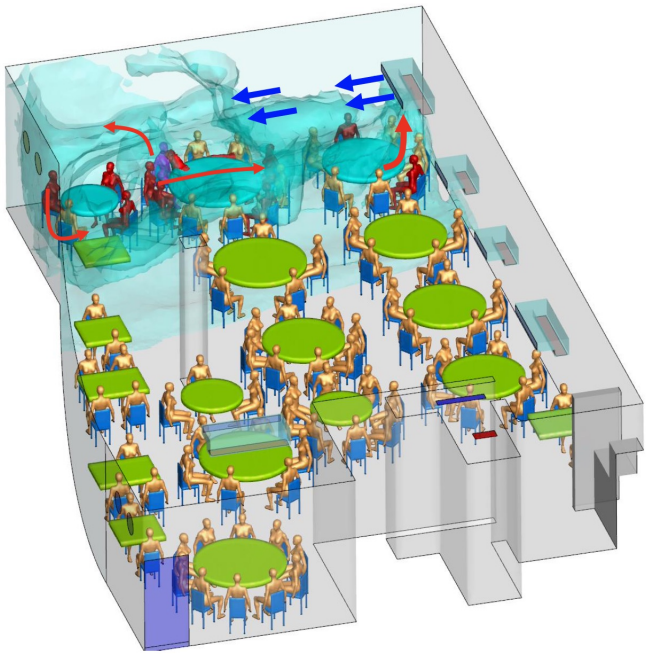

Figure 5: A CFD simulation of the contagion in the restaurant in Guangzhou China. The blue gas models the contamination by the droplet/aerosols. The infected people are colored red. Notice that the contaminated region roughly forms a pyramid with base on the wall opposite to the air-conditioner. The figure is take from [16].

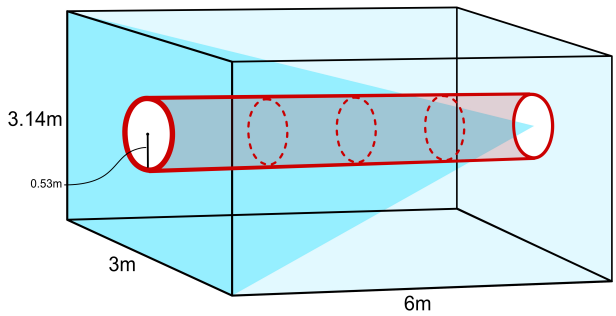

Figure 6: A cartoon (not to scale) of the volume (red cylinder) where the droplet/aerosol clouds propagate and the volume (blue pyramid) that the droplet/aerosol clouds get spread to my the air-conditioning.

4 Discussion

In [17] it was speculated that the flow generated by the air-conditioning was blowing large droplets from table to table. This is highly unlikely since the air-conditioning flow (0.25 m/s) does not have enough energy to send the droplets on a ballistic trajectory between the tables. In [16] the blame for the outbreak was put on the poor air-conditioning in the restaurant, caused by the closed vents and small injection of fresh air. So we redid the simulation with the recommended [1] injection of fresh air 8 liters per second for each person in the infected area. There are 21 persons at the three tables A, B and C and during the 4 minutes it takes the infected person to fill the cylinder above with a droplet/aerosol cloud, 40,320 liters or 40.32 m^3 are injected into the infected area, if the air-conditioning follows recommendations. Adding this to the total volume above we get 96.84 m^3, 32.28 m^3 of which pass through the pyramid containing the infected air. The concentration is decreased by a factor of 6.06 and in one hour we get 15 times 1/6.06 = 2.48 fold increase in concentration. This means that the concentration increases to what it would be next to the infected person in 25 minutes, in one hour it is almost 2.5 times that. Thus fixing the air-conditioning, that was present, does not solve the problem. We also asked the question how much injection of fresh air would we need to prevent the build-up in the droplet/aerosols? If we increase the injection to 80 l/s per person in the infected area, the simulation give us as reduction of 1/2 per hour. In other words, in one hour each person only experiences 1/2 of the concentration it would experience if he or she was sitting next to the infected person. In [20] the transmission of the virus droplet/aerosol through an air-conditioning system is discussed with the conclusion that greater volume of outdoor air and MERV-13 or HEPA filters with the capacity of filtering our the droplet/aerosols need to be used. This is consistent with our observations. However, the air-conditioners in current use may be unable to use MERV-13 filters or handle the required volume of outdoor air. Indeed a new generation of air-conditioners that meet these requirements may be needed.

A The Richardson Scaling

Diffusion of droplets or particles was modeled by Richardson [21] who assumed that the diffusivity is,

$$D_R = \frac{d\langle r^2\rangle}{dt} = k_0 \varepsilon^{1/3} \langle r^2\rangle^{2/3},$$

based on empirical evidence where $r(t)$ is the particle separation at time t. The solution of this equation gives

$$\langle r^2(t)\rangle = g\,\varepsilon\,t^3,$$

where $g = k_0^3/27$ is called the Richardson constant. This is know as Richardson diffusion. Obukhov [19] gave a derivations based on the Kolmogorov-Obukhov scaling

$$D_R = \frac{d\langle r^2\rangle}{dt} = \tau(r)\langle(\delta u)^2\rangle,$$

where δu is the Lagrangian velocity difference, so $\langle(\delta u)^2\rangle$ is the second Lagrangian structure function and $\tau(r)$ is the eddy turnover time. Now according to the Kolmogorov-Obukhov Theory,

$\langle(\delta u)^2\rangle = C_2\varepsilon^{2/3}r^{2/3}$ and $\tau(r) = \varepsilon^{-1/3}r^{2/3}$, so

$$\frac{d\langle r^2\rangle}{dt} = \tau(r)\langle(\delta u)^2\rangle = C_2\varepsilon^{1/3}r^{4/3}.$$

The solution is

$$\langle r^2(t)\rangle = \frac{C_2}{27}\varepsilon\, t^3,$$

or $g = \frac{C_2}{27}$. This holds for $\eta << r_0 < \langle r^2(t)\rangle^{1/2} << L$, where η is the Kolmogorov constant and L is the system size. r_o is the initial particle separation.

In addition to this region, there is a ballistic regime derived by Batchelor [4]. In this regime the particles separate linearly in t depending on the initial velocity. For the initial separation of the particles r_0 very small, first there is a ballistic region and at a later time the particles separate exponentially. This marks the beginning of the Richardson diffusion.

We assume that the droplet/aerosols are passive scalar, or that they are simply carried along by the flow without influencing the flow itself. The probability density function, for the separation r of the passive scalars, satisfies the partial differential equations (PDE)

$$\partial_t P(r,t) = r^{-2}\partial_r r^2 C_{||}(r)\partial_r P,$$

where $C_{||}$ is the longitudinal correlation function. With $C_{||} \sim Dr^{4/3}$ and $P_0(r,t_0) = \delta(t-t_0)$, the PDE has an explicit solution in the large time limit, see [15] and [3],

$$P_{Ric}(r,t) \approx \frac{r^2}{\langle r^2(t)\rangle^{3/2}} \exp\left(-d(\frac{r}{\langle r^2(t)\rangle^{1/2}})^{2/3}\right),$$

where d is a constant determined by D. This assumes that the velocity field is stochastic, incompressible, homogeneous and isotropic and δ correlated in time.

The Richardson scaling allows us to express the Richardson probability density function (PDF) in terms of the structure functions. Namely, using the above to set $r^2 = \frac{C_2}{27}\varepsilon t^3$, we get that $\tilde{C}_2 = C_2^{4/3}/3$, and

$$\langle(\delta u)^2\rangle = C_2\varepsilon^{2/3}r^{2/3} = \frac{C_2^{4/3}}{3}\varepsilon t,$$

so

$$\langle r^2(t)\rangle = \frac{1}{C_2^3\varepsilon^2}\langle(\delta u)^2\rangle^3.$$

A substitution into the PDF above gives

$$P_{Ric}(r,t) \approx \frac{C_2^{9/2}\varepsilon^3 r^2}{\langle(\delta u)^2\rangle^{9/2}} \exp\left(-\frac{9}{4}\frac{\varepsilon^{2/3}C_2 r^{2/3}}{D\langle(\delta u)^2\rangle}\right), \tag{A.1}$$

using the value $d = \frac{9}{4D}$ from [3]. D is the coefficient in the Richardson law

$$r^{2/3} = \frac{2}{3}Dt = \frac{C_2^{1/3}}{3}\varepsilon^{1/3}t,$$

so $D = \frac{1}{2}\varepsilon^{1/3}C_2^{1/3}$.

B Computation of the Richardson Coefficient

The second Lagrangian structure function is

$$S_2(r,t) = \frac{4}{C^2}\sum_{k\in\mathbb{Z}\setminus 0}\Big[\frac{\frac{C}{2}c_k(1-e^{-2\lambda_k t})}{|k|^{2/3}+\frac{4\pi^2\nu}{C}|k|^{2/3+\frac{4}{3}}}+\frac{|d_k|^2(1-e^{-\lambda_k t})}{|k|^{2/3}+\frac{8\pi^2\nu}{C}|k|^{2/3+\frac{4}{3}}+\frac{16\pi^4\nu^2}{C^2}|k|^{2/3+\frac{8}{3}}}\Big] \times(|\sin^2(\pi k\cdot r)|),$$

by the stochastic closure theory, see [7]. At $t=\infty$ and for r small we get

$$S_2(r,\infty) = \frac{4\pi^{2/3}}{C^2}\sum_{k\in\mathbb{Z}\setminus 0}\Big[\frac{\frac{C}{2}c_k}{1+\frac{4\pi^2\nu}{C}|k|^{\frac{4}{3}}}+\frac{|d_k|^2}{1+\frac{8\pi^2\nu}{C}|k|^{\frac{4}{3}}+\frac{16\pi^4\nu^2}{C^2}|k|^{\frac{8}{3}}}\Big]\, r^{2/3}$$

$$= \frac{4\pi^{2/3}}{C^2}\sum_{k\in\mathbb{Z}\setminus 0}\Big[\frac{\frac{C}{2}b^2}{(b^2+|k|^m)^2}\frac{1}{(1+\frac{4\pi^2\nu}{C}|k|^{\frac{4}{3}})}+\frac{a^2}{(a^2+|k|^m)^2}\frac{1}{(1+\frac{8\pi^2\nu}{C}|k|^{\frac{4}{3}}+\frac{16\pi^4\nu^2}{C^2}|k|^{\frac{8}{3}})}\Big]\, r^{2/3},$$

where we have used the models $c_k=\frac{b^2}{(b^2+|k|^m)^2}$ and $d_k=\frac{a^2}{(a^2+|k|^m)^2}$ from [14], for the coefficients c_k and d_k.

The Taylor-Reynolds number for the restaurant in Guangzhou is $Re_\lambda = 705$, the distance from the infected person to the wall with the air-conditioner is 3 meters, the air velocity in that direction is 0.25 m/s. The parameters C,a,b and m depend on the Reynolds number, we interpolate them from the values computed in [14], to get $C=5.574$, $a=6.508$, $b=0.076$ and $m=1.000$. The value of $\varepsilon=1.2$ is obtained from [6] at $Re_\lambda=690$, this is close to our value of 705. With this information we can compute the coefficient C_2 in the structure function $S_2(r)=C_2(705)r^{2/3}$, namely

$$C_2 = \frac{4\pi^{2/3}}{5.574^2}\sum_{k\in\mathbb{Z}\setminus 0}\Big[\frac{2.787\times 0.076^2}{(0.076^2+|k|)^2}\frac{1}{(1+\frac{4\pi^2\nu}{5.574}|k|^{\frac{4}{3}})}+\frac{6.508^2}{(6.508^2+|k|)^2}\frac{1}{(1+\frac{8\pi^2\nu}{5.574}|k|^{\frac{4}{3}}+\frac{16\pi^4\nu^2}{5.574^2}|k|^{\frac{8}{3}})}\Big] = 0.489.$$

This gives the exponent in the Richardson PDF,

$$d=\frac{9}{4D}=\frac{9}{2C_2^{1/3}\varepsilon^{1/3}}=5.376.$$

Acknowledgements: The first author wants to thank Klaus Schauser and Albert Oaten for enthusiastic support and Ken Beisser for expert advice on air-conditioning. We also thank Knut Bauer for providing us with the graphic illustration in Figure 6.

References

[1] ANSI/ASHRAE Standard 62.1. *Ventilation for acceptable indoor air quality*. 2019.

[2] L. Angheluta and B. Birnir. The velocity structure functions in Lagrangian turbulence. *To appear*, 2020.

[3] E Balkovsky and V Lebedev. Instanton for the kraichnan passive scalar problem. *Physical Review E*, 58(5):5776, 1998.

[4] G. K. Batchelor. *The Theory of Homogenous Turbulence*. Cambridge Univ. Press, New York, 1953.

[5] G. K. Batchelor. *Homogeneous Turbulence*. Cambridge University Press, 1960.

[6] Luca Biferale, Eberhard Bodenschatz, Massimo Cencini, Alessandra S Lanotte, Nicholas T Ouellette, Federico Toschi, and Haito Xu. Lagrangian structure functions in turbulence: A quantitative comparison between experiment and direct numerical simulation. *Physics of Fluids*, 20(6):065103, 2008.

[7] B. Birnir. The Kolmogorov-Obukhov statistical theory of turbulence. *J. Nonlinear Sci.*, 2013. DOI 10.1007/s00332-012-9164-z.

[8] B. Birnir. *The Kolmogorov-Obukhov Theory of Turbulence*. Springer, New York, 2013.

[9] B. Birnir, L. Angheluta, J. Kaminsky, and X. Chen. Spectral link of the Generalized Townsend-Perry constants in turbulent boundary layers. *Physical Review Research*, Submitted, 2020.

[10] Björn Birnir. *From Wind-Blown Sand to Turbulence and Back*, pages 15–27. Springer International Publishing, Cham, 2016.

[11] L. Bourouiba. Turbulent gas clouds and respiratory pathogen emission, potential implications for reducing transmission of covid-19. *JAMA Insights*, 2020.

[12] Lydia Bourouiba, Eline Dehandschoewercker, and John WM Bush. Violent expiratory events: on coughing and sneezing. *Journal of Fluid Mechanics*, 745:537–563, 2014.

[13] G. Gioia, N. Guttenberg, N. Goldenfeld, and P. Chakraborty. Spectral theory of the turbulent mean-velocity profile. *Physical Review Letters*, 105, 2010.

[14] J. Kaminsky, B. Birnir, G. Bewley, and M. Sinhuber. Reynolds number dependence of the structure functions in homogeneous turbulence. *Journ. of Nonlin. Sci.*, pages 1–34, 2020.

[15] R. H. Kraichnan. Lagrangian-history closure approximation for turbulence. *Phys. Fluids*, 8:575–598, 1965.

[16] Yuguo Li, Hua Qian, Jian Hang, Xuguang Chen, Ling Hong, Peng Liang, Jiansen Li, Shenglan Xiao, Jianjian Wei, Li Liu, et al. Evidence for probable aerosol transmission of sars-cov-2 in a poorly ventilated restaurant. *medRxiv*, 2020.

[17] Jianyun Lu, Jieni Gu, Kuibiao Li, Conghui Xu, Wenzhe Su, Zhisheng Lai, Deqian Zhou, Chao Yu, Bin Xu, and Zhicong Yang. Covid-19 outbreak associated with air conditioning in restaurant, guangzhou, china, 2020. *Emerging Infectious Diseases*, 26(7), 2020.

[18] AS Monin and AM Yaglom. Mechanics of turbulence. *Statistical fluid mechanics*, 2, 1975.

[19] A Obukhov. Spectral energy distribution in a turbulent flow. *Izv. Akad. Nauk. SSSR. Ser. Geogr. i. Geofiz*, 5:453–466, 1941.

[20] PENG Renat Manassypov PHD. Evaluating virus containment efficiency of air-handling systems. *ASHRAE Journal*, 62(7):17–23, 2020.

[21] Lewis Fry Richardson. Atmospheric diffusion shown on a distance-neighbour graph. *Proceedings of the Royal Society of London. Series A, Containing Papers of a Mathematical and Physical Character*, 110(756):709–737, 1926.

[22] BE Scharfman, AH Techet, JWM Bush, and L Bourouiba. Visualization of sneeze ejecta: steps of fluid fragmentation leading to respiratory droplets. *Experiments in Fluids*, 57(2):24, 2016.

[23] Federico Toschi and Eberhard Bodenschatz. Lagrangian properties of particles in turbulence. *Annual review of fluid mechanics*, 41:375–404, 2009.

[24] A. A. Townsend. *The Structure of Turbulent Shear Flow*. Cambridge University Press, 1976.